Quantum chemical study of the effect of precursor stereochemistry on dissociative chemisorption and surface redox reactions during the atomic layer deposition of the transition metal copper

*Gangotri Dey, Simon D. Elliot**

***Corresponding author**: Tyndall National Institute, University College Cork, Dyke Parade, Cork, Ireland, email: simon.elliott@tyndall.ie, Tel: +353 21 490 4392, Fax: +353 21 490 4058

Abstract

Using quantum chemical calculations, we investigate surface reactions of copper precursors and diethylzinc as the reducing agent for effective Atomic Layer Deposition (ALD) of Cu. The adsorption of various commonly used $Cu^{(II)}$ precursors is explored. The precursors vary in the electronegativity and conjugation of the ligands, and flexibility of the whole molecule. Our study shows that the overall stereochemistry of the precursor governs the adsorption onto its surface. Formation of different $Cu^{(II)}/Cu^{(I)}/Cu^{(0)}$ intermediate complexes from the respective $Cu^{(II)}$ compounds on the surface is also explored. The surface model is a (111) facet of a Cu_{55} cluster. $Cu^{(I)}$ compounds are found to cover the surface after the precursor pulse, irrespective of the precursor chosen. We provide new information about the surface chemistry of Cu(II) versus Cu(I) compounds. A pair of CuEt intermediates or the dimer Cu_2Et_2 reacts in order to deposit a new Cu atom and release gaseous butane. In this reaction,

two electrons from the Et anions are donated to copper for reduction to metallic form. This indicates that a ligand exchange between the Cu and Zn is important for the success of this transmetallation reaction. The effect of the ligands in the precursor on the electron density before and after adsorption onto the surface has also been computed through population analysis. In the $Cu^{(I)}$ intermediate, charge is delocalized between the Cu precursor and the bare copper surface, indicating metallic bonding as the precursor densifies to the surface.

Keywords: Cu, ALD, $ZnEt_2$, $Cu^{(I)}$ compounds, geometry, adsorption onto the surface, .

I. Introduction

Copper has low electrical resistivity and a high electromigration resistance[1]. For this reason it is used as the material for electronic interconnects. Previously Al was used as interconnect and the change to Cu caused a radical change in the back end of line process. Hence, the damascene process[2] was introduced, where copper is electrochemically deposited onto an underlying seed layer[1a] by filling of narrow features. The seed layer should be ~2 nm thick and for adequate conductivity, it should be a continuous film. The Atomic Layer Deposition (ALD) technique can in principle be used to deposit this seed layer, but Cu tends to agglomerate into islands rather than forming a uniform continuous film[3]. The International Technology Roadmap for Semiconductors (ITRS)[4] regards the formation of a sufficiently thin seed layer as one of its main challenges for the upcoming years.

ALD is a unique nanofabrication technique where for many materials a uniform layer of a desired thickness can be deposited, provided suitable precursor compounds are found. The ALD method relies on alternate pulsing of the precursor gases onto the substrate surface causing chemisorption with the surface atoms. This is followed by purging away excess precursor molecules from the surface. The same reaction is repeated for the second set of co-reagents. This leads to surface reaction of the two compounds, generating the desired material and forming by-products. S. George *et al.* review[5] the basic concepts of ALD.

Many attempts have been made to develop an ALD process for copper metal using existing copper precursors. Various combinations of copper precursor and reducing agent have been tried. $Cu(hfac)_2$ and alcohol (hfac = 1,1,1,5,5,5-hexafluoro-3,5-pentanedionate)[6] at 300°C, CuCl and hydrogen as the reducing agent[7] at $T > 360$°C, $Cu(thd)_2$ and hydrogen at 260°C[8] (thd = 2,2,6,6-tetramethyl-3,5-heptanedionate) are three ALD processes that allow deposition of Cu at relatively high temperatures. However, one of the main requirements for Cu deposition is that the ALD process operates at a low reaction temperature ~100°C. A three step deposition technique was developed by Knisley *et al.*[9] using $Cu(dmap)_2$ as the precursor and formic acid and hydrazine for further reduction (dmap = $OCHMeCH_2$-NMe_2). Indirect methods like reduction of CuO by isoproponal[10], Cu_2O by formic acid over ruthenium[11] and Cu_3N by H_2[12] have also been tried. Kalutarage *et al.*[13] have reported the use of $BH_3(NHMe_2)$ as a new reducing agent along with alkoxides of first row transition metals. $Cu^{(I)}$amidinate compounds were described by Li *et al.*[14] as promising precursors for Cu ALD. However, later through the study of Ma *et al.*[15] it has become apparent that these reactions resemble thermal CVD rather than ALD. This indicates that $Cu^{(I)}$ molecules have a tendency to decompose at the surface.

Lee *et al.*[16] used the organometallic reagent diethylzinc ($ZnEt_2$) as a reducing agent and $Cu(dmap)_2$ as the precursor for $Cu^{(0)}$ deposition via transmetallation according to equation 1.

$$Cu(dmap)_{2(g)} + ZnEt_{2(g)} \rightarrow Cu_{(s)} + Zn(dmap)_{2(g)} + butane_{(g)} \quad \ldots.(1)$$

They reported low temperature ALD at around 100°C. The Cu layers were reported to be uniform, thin, conformal and without any contamination. The reaction was self-terminating, and so was used to coat patterned octadecylsiloxane self-assembled monolayers. Similar transmetallation reactions are used for the preparation of non-aqueous metal colloids[17].

The work of Lee *et al.* was followed by that of Vidjayacoumar *et al.*[18] who checked triethylborane and trimethylaluminium as alternative reducing agents in solution. They came

to the conclusion that diethylzinc is the best of the three reducing agents for copper deposition. But there was 10% deposition of zinc along with copper resulting in formation of brass rather than pure copper metal.

A gas-phase model was used by Dey *et al.*[19] to propose probable reactions that might take place during transmetallation ALD. Here $ZnEt_2$ was considered as the reducing agent. Broadly the overall transmetallation reactions were broken down into disproportionation, ligand exchange and reductive elimination. It was found that copper and zinc reaction energies were comparable and hence, it is inevitable that there is co-deposition of zinc along with copper. The pathway by which $Cu^{(0)}$ can be deposited was found to be the disproportionation reaction of the $Cu^{(I)}{}_2Et_2$ compound. This indicates that ligand exchange between the two metals (Cu and Zn) is very important as a way to bring Cu and Et together. The paper mentioned that similar type of ligands have similar features and can be grouped together. $Cu^{(I)}{}_2L_2$ (L = ligand) compounds play a crucial role in understanding the mechanism. This is because after the precursor pulse, the copper compounds always tend to form these $Cu^{(I)}$ compounds. The paper also mentioned other side reactions that might take place.

However, ALD is predominantly a surface phenomenon and the gas phase model could only give a view of probable reactions that might take place at the surface. Finding a stable intermediate species on the surface indicates a pathway for the ALD reactions. Computed adsorption energies of the different species are a measure of their relative stability, thus revealing the dominant surface compounds that can be found after different ALD pulses. In some cases, the gas phase reactions show exothermic reaction energies, indicating a probable pathway for the reaction mechanism, but the same reactions might not take place on the surface due to slow kinetics, lack of interaction between the intermediates or a strong substrate effect.

The mechanism of a reaction is the atomically-resolved pathway that is followed by the reactants in order to form the products via the intermediates. It is important to understand the mechanism in order to determine the kinetics, possible side reactions and also impurities. ALD reaction mechanisms have been studied in many cases. For example, Mui[20] *et al.* studied silicon nitride formation using a cluster model, Elam[21] *et al.* studied ALD of ZrO_2 using *in situ* mass spectrometry and first principle calculations, Heyman[22] studied different cycles in ALD of Al_2O_3 using $AlCl_3$ and H_2O, Leskela[23] and co-workers studied ALD of Ru and Pt using an *in situ* quadrupole mass spectrometer (QMS) and a quartz crystal microbalance (QCM) and Widjaja[24] *et al.* studied ALD of HfO_2 from $HfCl_4$ and H_2O using first principle calculations.

Ab initio calculations can give valuable insights into the mechanism of ALD reactions[25]. Short-lived intermediates can also be studied using these calculations, which might not be possible through experiments[26]. In most of the cases, Density Functional Theory (DFT) has been the preferred level of computation, because it provides a reliable description of chemical reactions at reasonable computational cost. It is computationally cheaper than other first principle techniques like Møller–Plesset second order perturbation theory or Coupled Cluster[27] and so allows larger systems to be computed. Computational study builds a bridge between the theoretical understanding and experimental data for various chemical reactions in ALD.

The ligand in the precursor plays a crucial role in ALD mechanism. It dictates the volatility of the precursor, surface adsorption and densification on the surface. Computing surface adsorption shows the structures of the precursors on the surface. Densification is defined as the increase in density due to improved metal (M) and ligand (L) M-L packing, associated with an increase in coordination numbers of metal and ligand[28]. Although densification has been shown to be important in ALD of oxides[29], it has hardly been discussed before for

metals[25]. The computed adsorption structures for Cu compounds show the densification that can take place for this metal.

In our current work, we use a surface model to study the cycles in Cu ALD during the transmetallation reaction as proposed in equation 1 (Figure 1). We compare various copper(II) precursors and consider $ZnEt_2$ as the reducing agent. Each ALD cycle comprises a precursor pulse and a co-reagent pulse[30]. Different surface reactions take place during each pulse. During a precursor pulse (denoted as pulse 1), the copper complexes CuL_2 come onto a surface covered with Et ligands from the previous co-reagent pulse. During the reducing agent pulse (denoted as pulse 2), $ZnEt_2$ comes onto a surface already covered with ligands (L) from the precursor. Thereafter, during either or both pulses, reactions may take place at the surface between ligands and Et groups and volatile by-products may be produced. After saturation has been reached, a particular type of ligand always dominates the surface.

In order to study these reactions, we have divided them into parts as shown in Figure 1. Each ALD pulse is conceptually broken into parts ‘a’ and ‘b’. Based on our prior study of this system[19], we expect that the following reactions take place in part 1a where co-reagent is present at the surface.

- Ligand exchange between the two metals (Cu/Zn).
- Formation of half and fully ligand exchanged Cu and Zn surface intermediates like LZnEt and LCuEt and volatile products like ZnL_2 and butane.
- Further reactions and decomposition of these intermediates.
- Formation of new Cu surface layer.

In part 1b, we study the system when an excess of the copper precursor is admitted to the bare copper surface without any co-reagent left. The following reactions are expected to take place.

- Adsorption of unreacted Cu precursors onto a bare surface.

- Dissociation of the copper precursor on the surface.

Part 2 deals with the reactions during the reducing agent pulse. All the reactions that take place in 1a are also expected to take place in 2a. However, in this case the surface is initially covered with precursor ligand (L).

In part 2b, the following reactions are expected to take place.

- Adsorption of $ZnEt_2$ onto a bare copper surface.
- Reaction of Et ligands with surface Cu atoms.

The transition from part 'a to b' in both pulses '1 and 2' is marked by the formation of a new copper layer. In pulse 1, copper deposits from the copper precursor and in pulse 2, copper deposits from the Cu(I) intermediates. This course of the reaction is cyclic as seen in the following:

1a → $Cu_{new\text{-}layer}$ → 1b →2a →$Cu_{new\text{-}layer}$ →2b →1a …….

In this paper we will study the reactions in parts 1b and 2b that take place on a bare copper surface. This can be assumed to be the situation in the latter half of every pulse after complete exhaustion of the other ligand. For this reason we start from a bare Cu surface and study the adsorption of each precursor and the stability of $Cu^{(I)}$ intermediates[25] at the surface stable adsorbates as they are an important prerequisite for growth as otherwise the unreacted precursor complex will be expelled out of the reactor. Just as important, Cu-containing surface intermediates should not desorb and other by-products should desorb cleanly so as to avoid impurities in the film. We therefore compute the adsorption/desorption energies of the copper precursors CuL_2, intermediate compounds Cu_2L_2 and by-products ZnL_2, Et-Et and L-Et . The potential energy change for the transformation from $Cu^{(II)}$ to $Cu^{(I)}$ for three different ligands is also studied. These are all the possible reaction steps that may be followed in part 1b of the pathway for $Cu^{(0)}$ deposition.

For part 2b of the ALD cycle, we study the interaction of $ZnEt_2$, the reducing agent, with a bare copper surface. This takes place when all the surface bound ligands from the precursors have interacted with the incoming $ZnEt_2$ compounds and have been eliminated. The excess $ZnEt_2$ that is present may then interact with the newly formed bare copper surface.

Our aim is to screen many reactions and precursors and map out the likely pathway from the thermodynamic reaction energies. Given the large number of possible species, we do not consider the kinetics of competing reaction steps and so no transition states have been computed in this study.

II. Methods

We have used first principles Density Functional Theory as implemented in the TURBOMOLE 5.8 program[31]. The Perdew-Burke-Ernzerhof (PBE)[32] functional was used with the resolution of identity (RI) approximation[33]. A valence double zeta with polarization basis set denoted by def-SV(P)[33a] was used for all electrons. We used the larger triple zeta basis set TZVPP[34] and dispersion functional D3[35] to check the accuracy of the level of calculation in a previous study[36]. It was seen that energy difference changed by 4-8%, especially when using the dispersion functional D3. However, the computational cost of these calculations was much higher and the qualitative results in terms of reaction mechanism were not affected. Therefore, due to its adequate accuracy, we have used the PBE/def-SV(P) method in this study.

An fcc Cu_{55} cluster, which is in the shape of a coin with (111) faces, was taken as a surface model. The bare cluster has C_{3v} symmetry (Figure 2). The copper coin is an open shell doublet system with a HOMO - LUMO energy difference of 1.8 kJ/mol. The Cu(II) precursors are open shell doublets. Therefore, all the calculations with adsorbate on the cluster were open shell triplet calculations computed within the unrestricted DFT formalism

with negligible spin contamination. This is the same model as used by Larsson *et al.*[37] and in our previous studies[36, 38]. There are few studies done previously of organic and organometallic adsorption onto a copper surface by Crispin *et al.*[39].

Some of the adsorbates cover the entire copper surface and overlap the edges of the cluster. However, a bigger cluster is computationally very expensive. The edge effect that arises is already discussed in our previous study[36]. Correcting for this gives an energy difference of ~8% and the qualitative adsorption energies do not change. Hence, the adsorption energies quoted in this work have an error limit in this range.

In this paper we have focused on the surface reactions of copper precursors onto a copper surface. After ligands have been removed during each pulse of the ALD cycle it is assumed that there is a new layer of bare copper and that any incoming precursors will react with this new copper surface. Such a surface is likely to occur in its most stable geometry at the scale of individual precursor molecules (although it is known that islanding occurs at longer scales) and hence, we choose the most stable smooth copper surface for our study, Cu(111).

A comparative study of the reactive adsorption of the more commonly used $Cu^{(II)}$precursors onto the surface has been carried out. The precursors are copper$^{(II)}$acetylacetonate $Cu(acac)_2$, copper$^{(II)}$pyrrolylaldehyde $Cu(PyrAld)_2$, copper$^{(II)}$N-isopropyl-2-pyrrolylaldiminate $Cu(PyrIm^{iPr})_2$, copper$^{(II)}$dimethylamino-2-propoxide $Cu(dmap)_2$ and copper$^{(II)}$-bis(4N-(ethylamino)pent-3-en-2-onate commonly known as AbaCus$^{(TM)}$. The precursors vary in the electronegativity of the ligating atom, π conjugation present in the ligands and also steric hindrance in the coordination shell (Figure 3).

The energy of adsorption of the precursors to the bare surface has been calculated by this equation:

$$\Delta E_{ad} = E(\text{Pre+Coin}) - E(\text{Coin}) - E(\text{Pre}) \quad \ldots(4)$$

where E(Pre+Coin) denotes the total energy of the optimized geometry of the copper precursor adsorbed onto the bare copper surface, E(Coin) denotes the total energy of the optimized bare copper surface model, and E(Pre) denotes the total energy of the relaxed copper precursor in the gas phase.

The entropy of the precursor molecules S(Pre) has also been calculated in the gas phase from vibrational analysis using TURBOMOLE[40]. The entropy has been calculated at T = 393 K as this is a typical target temperature for Cu ALD. After the precursor is adsorbed onto the surface, it loses its translational and rotational degrees of freedom and this is probably the major contribution to the entropy change. It is therefore assumed that S(Pre+Coin) ≈ S(Coin) + S_{vibr}(Pre) and so the entropy change is $\Delta S_{ad} \approx -S_{trans+rot}$(Pre). $\Delta G_{ad} = \Delta E_{ad} - T\Delta S_{ad}$ denotes the free energy needed by the precursors to be adsorbed onto the surface. A lower more negative ΔG_{ad} value for the precursors indicates that the adsorption is favored. Likewise a higher more positive value for the by-products means that desorption is favored. The change in molecular structures from the free to the adsorbed state is also noted. *Ab initio* Molecular Dynamics (aiMD) using the same PBE functional and def-SV(P) basis set has been conducted on the $ZnEt_2$ molecule from an initial temperature of 393 K within the isothermal and isobaric ensemble. The total duration of the aiMD simulation was 2.17 ps.

All the precursors feature copper in formal oxidation state II and some of the surface intermediates studied here like Cu_2L_2 have copper in the oxidation state I. However, population analysis has been carried out in order to understand the actual charge distribution in different structures. Natural Population Analysis (NPA)[41] has been chosen as it exhibits better numerical stability for compounds containing metal atoms than other methods like Mulliken population analysis[42]. Nevertheless we note that these results are subject to the systematic problem of approximate DFT in localizing electrons in partially occupied metal d states (e.g. $Cu^{(I)}$ vs $Cu^{(II)}$).

III. Results

This section is divided into four parts. In section III.a we study the copper precursor adsorption onto a bare copper surface for various precursors. In section III.b we study the stability of Cu_2L_2 compounds on the surface. In section III.c, we study the change in charge distribution of the copper compound, from the gas phase, to the adsorbed CuL_2 and Cu_2L_2 compounds. Section III.d considers the interaction of the $ZnEt_2$ with the bare copper surface. The initial three sections are relevant to part 1b of the ALD cycle and the latter section to part 2b.

III.a. Adsorption of copper precursors onto bare copper surface:

Five different precursors that differ in electronegativity of the ligating atom, π conjugative stability in the ligands and steric hindrance have been considered here. The comparison allows us to understand their adsorption onto a bare copper surface. A precursor that has strong adsorption is beneficial, as it will not be purged out of the reactor without first saturating the surface. Stronger adsorption energies of intermediates give an idea of the dominant species that can be present at any time during the ALD reaction.

- $Cu(acac)_2$ (Figure 3(i)) has O atoms in the ligand attached to the copper center. The ligand has conjugated O-C-C-C-O π system in which the negative charge is delocalized.
- $Cu(PyrAld)_2$ (Figure 3(ii)) has both N and O as ligating atoms and has conjugated bonds present in O-C-C-N fused to a pyrrole ring. It has a distorted tetrahedral structure about the Cu center. It has mirror symmetry across a horizontal plane through the copper center.

- $Cu(PyrIm^{iPr})_2$ (Figure 3(iii)) is similar to $Cu(PyrAld)_2$ except that (a) it has higher steric hindrance due to the presence of an isopropyl group attached to the imine nitrogen and (b) the electronegative atoms attached to the copper are N and N, not N and O as in the case of PyrAld.

- $Cu(dmap)_2$ (Figure 3(iv)) is different from the above precursors as the ligand does not have any conjugation present. Otherwise, it is comparable to $Cu(PyrAld)_2$ as it has 4-atom O-C-C-N ligating unit, but no fused ring. It does not have a mirror plane and ligating atoms are arranged anti around Cu.

- Copper-bis(4N-(ethylamino)pent-3-en-2-onate) $AbaCus^{(TM)}$ (Figure 3(v)) is a precursor that is similar to $Cu(dmap)_2$ but has conjugation present in its ligand. It does not have a mirror plane and ligating atoms are arranged anti around Cu.

The difference between gaseous and adsorbed structures is shown in Table 1 for copper precursors. The bond length between the metal Cu and the O/N atom in ligand, as well as the distance from the nearest surface copper atom is noted. When some of the precursors are adsorbed onto the coin, there is considerable change in metal-ligand bonding and the dihedral angle between the four ligating atoms. For example, the ∟O-N-O-N angle in $Cu(dmap)_2$ changes from 0.6° to 104°.

We see that the structure of the precursor affects the adsorption onto the surface. A planar complex like $Cu(acac)_2$ that is free of any bulky substituent, has better access to the surface copper atoms. There is partial transfer of the ligand from the complex to the surface, where the ligands form extra bonds with the surface copper atoms (Figure 4 (i)). The bond length between the Cu_{pre} (in the precursor) and ligand O lengthens from 1.95 Å to > 2.10 Å.

The $Cu(PyrAld)_2$ precursor is also free of steric hindrance from bulky substituents but it has an almost tetrahedral structure around Cu_{pre}. In order for the precursor to adsorb, the Cu_{pre}-O bond dissociates to a length of 2.61/2.72 Å, much longer than the normal Cu-O bond

found in an organometallic compound[43] (1.92 Å) (Figure 4 (ii)). The O remains unbonded to both Cu_{pre} and $Cu_{surf.}$

When the lowest energy isomer of $Cu(PyrIm^{iPr})_2$ is put onto a bare copper surface, it is seen in the calculations that it does not chemisorb. This is because of the bulky ^{i}Pr groups, which are on the opposite sides of the plane of the precursor compound (Figure 5). The steric hindrance is lower with an alternative isomer where the ^{i}Pr groups are on the same side of the plane (Figure 4(iii)). The difference in energy between the two gas phase isomers is 5 kJ/mol. We see molecular adsorption of the precursor only after the transformation.

$Cu(dmap)_2$ also shows molecular adsorption onto the surface. The ligand O atoms form extra bonds with the surface atoms (Figure 4(iv)). However, the Cu-ligand bonds of the precursor complex do not dissociate.

In AbaCus, (Figure 4(v)), the steric hindrance that arises from the Et group on imino N in the ligand does not hinder the adsorption. The Et groups occupy the space above the plane of the molecule while the Cu_{pre} atom adsorbs to the surface below. The O atoms in the precursor break from the Cu_{pre} and bond to the Cu_{surf}. The Cu_{surf}-O distances are 2.55 Å and 2.17 Å.

The computed energies for the adsorption of Cu precursors and desorption of the by-products are reported in Table 2. The data can be interpreted as in the following example. It is computed that $Cu(acac)_2$ has an adsorption energy of ΔE_{ad} = -258 kJ/mol at 0 K. However, it faces an energy of ΔG^{393}_{ad} = -79 kJ/mol at 393 K because of the entropy factor ΔS_{ad} = -0.5 kJ/mol.K and $T\Delta S_{ad}$ = -179 kJ/mol. A similar interpretation with different results can be made for all the complexes in Table 2. From these data we see that the less sterically hindered acac precursor has the highest ΔE_{ad}. This is followed closely by $PyrIm^{iPr}$, dmap and AbaCus precursors. The least negative ΔE_{ad} is for PyrAld. It is seen that, except for $Cu(PyrAld)_2$, all other precursor complexes show favorable adsorption at ALD temperatures, $\Delta G^{393}_{ad} < 0$.

Adsorption of $CuEt_2$ has also been explored as this compound might be formed after a ligand exchange with $ZnEt_2$. It is seen that ΔE_{ad} is strongest in this case as against any of the above precursors.

The Cu_{pre} forms a cap over copper surface after adsorption. The Cu_{pre} encircles three Cu_{surf} atoms (Figure 4 (i), (ii), (iii), (v)). This is seen for all precursors except dmap (Figure 4 (iv)) where the dmap bridges between two Cu_{surf}. The adjacent O atoms bind to the surface for acac, dmap and AbaCus. The O adsorbs onto the coordinately unsaturated copper surface. It is seen from Table 1 that the Cu-O bond always lengths more compared to Cu-N bond in precursor ligands, which have both (N, O) atoms like dmap, PyrAld etc.

III.b. Adsorbed Intermediates

It seems that $Cu^{(I)}{}_2L_2$ is an important intermediate that can be formed during the transmetallation reaction[18-19]. This stems from our previous study of the gas phase transmetallation reaction, where it was seen that after the precursor pulse, the surface is likely to be covered with these $Cu^{(I)}$ intermediates. Comproportionation of $Cu^{(II)}$ and $Cu^{(0)}$ to $Cu^{(I)}$ was found to be exothermic. However, the previous study did not explicitly consider surface reactions.

In the current study, we find that all Cu_2L_2 intermediates exist as molecules adsorbed on the surface. The theoretical adsorption energies of these intermediates are reported in Table 3 in order to assess their stability against desorption. The $Cu^{(I)}$ intermediates seem to release the strain present in the corresponding $Cu^{(II)}$ precursors (Table 2). The open structure of Cu_2L_2 allows better access for the $Cu^{(I)}$ centers to the surface Cu atoms for bonding. This allows stronger adsorption to the surface (Table 3).

We have previously identified three types of $Cu^{(I)}$ compounds[19]: in Cu_2L_2 each ligand is attached to two copper atoms; in CuL there is no Cu-Cu bond and each ligand is attached to only one Cu atom and in Cu_2L there is only one ligand attached to two copper atoms (Figure

6). In Cu_2L one of the Cu is formally in oxidation state zero and the other is in +1 oxidation state. In the current study, we find similar possibilities for $Cu^{(I)}$ adsorbates, validating the previous study (Figure 6).

Various reactions are possible for the $Cu^{(I)}$ intermediate. It can desorb from the surface or transform into another type of $Cu^{(I)}$ intermediate or else disproportionate into $Cu^{(II)}$ compounds and $Cu^{(0)}$. The computed energetics for these possibilities are shown in Figure 7 for L = dmap and Figure 8 for L = $PyrIm^{iPr}$. The desorption energies (ΔE_{des}) and free energies (ΔG_{des}) that include ΔS are also shown in the graphs. It is known that entropy always favors desorption. Hence, ΔG_{des} is always less than ΔE_{des} irrespective of the system studied. Conversion from one stable intermediate to another stable intermediate with a transition from a higher intermediate might indicate an activation barrier for this reaction. We see that amongst all the surface species, the $Cu^{(I)}$ intermediates are the most stable for all the ligands studied.

As seen in Figure 7 and Figure 8, the reaction energies for $Cu^{(II)}$ and surface $Cu^{(0)}$ atoms to comproportionate into $Cu^{(I)}$ are < -100 kJ/mol. Therefore, subject to overcoming the unknown kinetic barriers, the reaction is expected to take place. For the dmap ligand the most stable surface intermediates are $Cu^{(I)}{}_2L_2$ and Cu_2L (Figure 7) and for L = $PyrIm^{iPr}$, Cu_2L is the most stable (Figure 8). The desorption of the $Cu^{(I)}$ intermediates is not likely for the dmap ligand as the energies required are $\Delta G_{des}{}^{393}$ > 300 kJ/mol. However, $PyrIm^{iPr}$ compounds have more probability for desorption of the $Cu^{(I)}$ compounds ($\Delta G_{des}{}^{393}$ = -111 kJ/mol). This is because they show more tendency than dmap to retain the $Cu^{(I)}$ structure rather than $Cu^{(II)}$. This was seen in the gas phase studies as well[19]. However, $Cu^{(II)}L_2$ is energetically more likely to desorb than $Cu^{(I)}L_x$ in all the cases. Thus during step 1b of the copper precursor pulse, when all the pre-existing ligands from the reducing agent have been expelled from the system, the surface becomes covered with $Cu^{(I)}$ complexes.

III.c. Population Analysis of $PyrIm^{iPr}$, dmap and AbaCus precursors:

Table 4 shows the population analysis using NPA of three CuL_2 compounds before and after adsorption onto the surface. They are chosen such that the ligand varies in electronegativity (N, O as in dmap and AbaCus but N,N in $PyrIm^{iPr}$), flexibility in the precursor (conjugation in the ligands AbaCus, $PyrIm^{iPr}$ but no conjugation in dmap) and size of the ring including copper (five membered ring in dmap and $PyrIm^{iPr}$ but six membered ring AbaCus). For CuL_2 adsorption in all three cases, each ligand gains -0.3 negative charge on adsorption to the Cu (111) surface and the surface donates this amount of charge. The exception is for the second ligand in the $PyrIm^{iPr}$ precursor, which is an artifact of the calculation because the ligand is bound towards the edge of the copper cluster. The positive charge initially on the Cu atom in the precursor becomes shared between the surface and adsorbed Cu (Table 4). This delocalization may contribute to stabilization of the adsorbed copper complexes and can be interpreted as metallic bonding. The redistribution of charge over the copper surface is less for the Cu_2L_2 compound compared to CuL_2. The charge left on the two adsorbed Cu_2L_2 centers and the ligands are roughly the same, regardless of precursor. **Error! Reference source not found.** shows the charge difference for $Cu(dmap)_2$ precursor before and after adsorption to the copper surface.

III.d. Interaction of $ZnEt_2$ with a bare copper surface:

In this section, we explore the $ZnEt_2$ interaction with a bare copper surface. This takes place in an ALD chamber when there is an excess of the reducing agent and the previously-adsorbed ligands from the precursors are exhausted. This can be assumed to take place at the latter half of the reducing agent pulse (Figure 1, step 2b).

After finding the minimum energy structure of $ZnEt_2$ adsorbed on the copper surface, we have conducted an aiMD study of this adsorbate at typical ALD temperature. Within the

very short simulation time of 2.17 ps, we see that the adsorbate $ZnEt_2$ dissociates into ZnEt and Et fragments and that these two fragments attach themselves to the copper cluster. This might indicate no activation barrier for this reaction at this temperature. The bond distance between the Zn and the detached Et is 2.37 Å as opposed to 2.08 Å in $ZnEt_2$. Figure 10 shows the steps that take place in the above reactions. The adsorption of ZnEt to the copper surface (ΔE_{ad} = -264 kJ/mol) is computed to be stronger than that of $ZnEt_2$ (ΔE_{ad} = -115 kJ/mol) and so desorption of the ZnEt fragment is unlikely. The adsorption of ZnEt is even stronger than all the copper precursors studied here. Therefore, at the end of the reducing agent pulse we predict that there are fragments of Cu_{surf}-Et and ZnEt on the copper surface.

We suggest that Cu_{surf}-Et can undergo similar surface reactions as outlined for Cu-dmap and Cu-$PyrIm^{iPr}$ in the previous section (III.b). Therefore, we explore the stability of the Et ligand attached to $Cu^{(I)}$ or $Cu^{(II)}$ at the surface and desorption of the respective complexes. Figure 11 shows the graph for this study. Once again, various $Cu^{(I)}$ surface compounds are found to be more stable intermediates than those of $Cu^{(II)}$. Formation of $CuEt_2$ and its desorption is not favored. However, it is striking that in this case the deposition of $Cu^{(0)}$ and the desorption of butane from the surface is energetically favored (ΔE = -156 kJ/mol relative to two neighboring CuEt intermediates).

IV Discussion:

Through the above adsorption energies, we can assess whether adsorption of the precursors onto the surface plays an over-riding role in the overall process of Cu ALD. A weak adsorption of the compounds (e.g. $Cu(PyrAld)_2$) might indicate poor surface coverage. The energetics also show that auxiliary reactions that lead to the formation of Cu_2L_2 type surface compounds are inevitable in the precursor pulse. These are discussed below in sections IV.(a) and IV.(b). The interaction of the $ZnEt_2$ with the bare copper surface during the co-reagent pulse is discussed in the last section.

IV.(a). Adsorption of CuL_2 onto the surface:

The strength of adsorption (ΔE_{ad} in Table 2) for different copper precursors CuL_2 (L= ligand) onto the bare Cu (111) surface is computed to be in the following order:

L = Et>acac >dmap > $PyrIm^{iPr}$ > AbaCus>>PyrAld

We see that the entropy factor is of similar range for most of the precursor compounds (Table 2). Therefore, the difference between the adsorption energies ΔE_{ad} is primarily responsible for the difference between the free energies (ΔG^{393}_{ad}).

The factors determining ΔE_{ad} are discussed in the following paragraphs. The bond distance between the copper atom in the adsorbed precursor (Cu_{pre}) and the nearest copper atom in the surface (Cu_{surf}) follows the order (Table 1):

$PyrIm^{iPr}$>PyrAld>dmap >AbaCus> acac>Et.

The distances are in the range 2.37 Å – 2.72 Å. It might be expected that the adsorption is strongest for the precursor that has the shortest distance to the Cu_{surf}. However, comparing the two trends presented above, we see that this holds for the most strongly bound two compounds (Et and acac), but not for the rest. An alternative explanation might be the steric hindrance and the overall strain present in the precursor complex that hinders adsorption. The extra bonds formed between the precursor ligands and Cu_{surf} atoms after adsorption might also be important.

To examine this, we first consider the $Cu(acac)_2$ precursor. The complex is planar as expected for a $Cu^{(II)}$ compound[44]. The complex does not have any bulky substituents above or below the plane. In addition no inter-ligand interaction distorts the complex (Figure 3 (i)). This planar complex can thus easily approach the Cu(111) surface, allowing Cu_{pre} to access the surface Cu atoms. The favorable adsorption geometry is reflected in a short Cu_{pre} - Cu_{surf} distance and high ΔE_{ad} for $Cu(acac)_2$. Indeed, $Cu(acac)_2$ adsorbs dissociatively, forming strong bonds between the O (in the ligand) and Cu_{surf}. This might also contribute to its

stronger adsorption than the other precursors. However, formation of these extra bonds with the Cu_{surf} may be a disadvantage for the overall process, as it may be difficult for the ligand to be eliminated from the system. Hence, ΔG_{ad} of the precursor solely is not enough to determine the quality of the precursor and a detailed mechanistic study for the ligand exchange reactions is also important.

The lowest energy isomer of $Cu(PyrIm^{iPr})_2$ features bulky ligands (^{i}Pr) that point perpendicular to the plane of the precursor complex (Figure 3 (iii)). This brings in a high steric hindrance between the precursor molecule and the surface. This also distorts the $Cu^{(II)}$ complex out of the planar geometry (Table 1). The bulky substituents prevent the approach of the Cu_{pre} center to the surface and no adsorption geometry could be found. However, in the modified precursor (Figure **5**), one side of the complex is free of bulky substituents, which allows the Cu_{pre} to approach the surface and adsorb (Figure 4 (iii)). This example shows that steric hindrance between the precursor complex and the flat (111) surface is important for determining adsorption to the surface. It is likely that adsorption onto a rough or defective surface would be easier.

Adsorption energies for the $PyrIm^{iPr}$ and dmap precursors are comparable (Table 2). From its geometry the modified $PyrIm^{iPr}$ isomer (Figure 4 (iii)) seems to experience comparable steric hindrance to the dmap complex (Figure 4(iv)) during adsorption. This is because both these precursor molecules have flexible alkyl groups perpendicular to the plane of the complex that can be oriented away from the surface. The dmap ligand has two methyl groups attached to the amino nitrogen while $PyrIm^{iPr}$ has ^{i}Pr substitution on the imine nitrogen. Both the precursors show molecular adsorption onto the surface. However, the $PyrIm^{iPr}$ ligand is based on a conjugated π system, while dmap is not. This makes the dmap ligand more flexible than $PyrIm^{iPr}$. The dmap ligand thus forms extra bonds between O and the surface Cu atoms, without breaking that of Cu_{pre}-O which contributes to stronger adsorption. The Cu_{surf}-

Cu_{pre} distance is 2.72 Å for $PyrIm^{iPr}$ and 2.62 Å for dmap. The electronegativity of ligating atoms (N,N vs O,N) and the charge distribution of the two precursors is different (Table 4) but this does not seem to be the primary factor dictating the adsorption of the precursor. $Cu(dmap)_2$ precursors have been reported to undergo decomposition by β-hydride elimination[45], which is a pathway to uncontrolled CVD and not ALD. Hence, $Cu(dmap)_2$ type precursors should be used with caution when tested for ALD reactions.

AbaCus is a six membered complex with an ethyl group on the amino nitrogen. The substituents and the π conjugation affect the orientation of the ligands around the copper center, giving a torsional angle of 131° between the four ligating atoms in the gas phase. The ethyl substituents both point towards one side of the distorted plane of the complex, which makes the other side of the plane free for adsorption. The results are a short bond distance between the Cu_{surf} and Cu_{pre} atoms and new Cu-O bonds (Figure 4(v)). However, there is evidently substantial strain in the adsorbed complex, possibly because of distortion of the π system, as indicated by the lengthening of the Cu-O/N bonds by 0.5 Å, and the overall adsorption energy is low.

The PyrAld precursor has a torsional angle ~ 30° between the two ligands attached to the copper center. This is due to inter-ligand repulsion between H's of the two fused pyrrole rings in the two ligands (Figure 3 (ii)). This non-planarity makes it hard for the Cu_{pre} to approach the surface copper atoms. The O in the precursor does not bond to the surface copper atoms as it is a part of the fused ring. The five membered Cu-containing ring of the PyrAld complex increases the strain compared to the six membered AbaCus, although the torsional angle of AbaCus is greater than that of PyrAld. The Cu_{surf} – Cu_{pre} distance is 2.67 Å. The PyrAld complex remains poorly chemisorbed onto the surface (ΔE = -127 kJ/mol, Figure 4(ii)). When combined with entropy at typical temperatures, these computed energetics indicates that adsorption is not thermodynamically favored. The pyrrole ring does seem to affect the

adsorption structure of PyrAld and $PyrIm^{iPr}$ as in both cases there is a longer Cu_{pre} - Cu_{surf} bond with new ligand to surface bonds.

In a review paper Puurunen[46] has described the intrinsic advantage of less hindered precursor molecules for adsorption onto the surface. The author mentions that chemisorbed sterically crowded precursors can shield reactive sites at the surface from being accessible to other unreacted precursor molecules and that this may result in irregular growth of film. Thus, among the studied precursors, acac and dmap are expected to have the intrinsic quality of higher surface coverage compared to the other precursor compounds, leading to higher growth rate and better film quality in ALD.

The above discussion shows that access of the Cu_{pre} atom to the surface is the most important factor in chemisorption of these complexes. The tendency for $Cu^{(II)}$ complexes to be planar is therefore advantageous. However, when there are bulky ligands present, especially on the ligating electronegative atoms adjacent to the Cu atom, the gas-phase complex twists itself to form a tetrahedral structure. The metal center is then well encapsulated within the ligand shell, which makes it difficult for Cu_{pre} to access the surface[47] (e.g. $PyrIm^{iPr}$). In these cases the adsorption energy is low. In the other planar precursors, Cu_{pre} bonds to Cu_{surf} and we find that the ligating atoms can also bond to the surface metal atoms, contributing extra adsorption energy. The exception is when a fused pyrrole ring makes the ligand too rigid (PyrAld and $PyrIm^{iPr}$). This might be valid for precursor molecules of other metals too, particularly planar d^9 cations. Figure 12 summarizes how possible substitution sites in the precursor complex can affect the adsorption to the copper surface. The same can be concluded for precursors of other metals.

The adsorption free energies (Table 1, ΔE_{ad}) for the copper precursors to the bare copper surface indicate strong bonding between most complexes and the surface. Strong bonding may in principle be due to ionic, covalent or metallic bonding and it seems that all

three contribute to this case, giving rich behavior that varies with precursor stereochemistry. The additional effect of dispersion interaction certainly merits future study. Focusing on the metallic Cu_{pre}-Cu_{surf} interaction, this may be interpreted as a move towards higher coordination for Cu_{pre} as it chemisorbs. This is therefore another example of densification as a key driving force during ALD reactions. Zydor *et al.*[48] have simulated the effect of a bulky ligand in the $Ti(CpMe_5)(OMe)_3$ and H_2O ALD process that explains the experimentally observed lack of ALD of the oxide as due to the inability of the hindered Ti center to chemisorb on the substrate. Here we observe similar results but for Cu precursors and ALD of metals. Thus, our study shows that the most sterically hindered precursors do not chemisorb to the surface and so may not participate in all subsequent reactions that lead to metal ALD.

IV.(b). Non-ALD reactions of Cu_2L_2:

Regardless of the ligand, $Cu^{(I)}$ compounds are computed to have stronger adsorption (Table 3) to the surface than $Cu^{(II)}L_2$ (Table 2). This means that desorption of the $Cu^{(I)}$ intermediates is less likely. The potential energy diagrams illustrate this point (Figure 7, Figure 8 and Figure 11). This is probably because of less steric crowding around the Cu_2 core compared to the corresponding $Cu^{(II)}$ precursor compound (Figure 6). The $Cu^{(I)}$ has better access to the surface copper atoms and the bond distance to Cu_{surf} is always lower than for the corresponding copper precursors. This is seen for all the ligands we have studied here. The ligand atoms also form extra bonds with the under-coordinated surface copper atoms, thus increasing the adsorption energy. There is no difference in charge distribution over the Cu atoms between ligands with and without conjugated π systems (Table 4).

The potential energy diagram is different for the two precursors (L = dmap in Figure 7 and L=$PyrIm^{iPr}$ in Figure 8). We see that the desorption energy for the various $Cu^{(I)}$ species is higher with the dmap ligand than with $PyrIm^{iPr}$. This is probably due to the flexibility present

in the dmap ligand, which allows the ligand to break from Cu_{pre} and bind to the surface copper atoms more strongly than its $PyrIm^{iPr}$ counterpart. The conjugation present in the $PyrIm^{iPr}$ ligand does not allow the ligand to form additional bonds with the surface atoms and so desorption of the complexes is easier, which would be determined for ALD.

The $Cu^{(I)}$ compounds are formed from the incoming $Cu^{(II)}$ precursors and $Cu^{(0)}_{surf}$ atoms, which means that surface $Cu^{(0)}_{surf}$ atoms are temporarily consumed in step 1b. However, in the subsequent $ZnEt_2$ pulse (step 2a), there is formation of intermediate CuEt or Cu_2Et_2, which decompose to form $Cu^{(0)}$ and butane (Figure 11). Likewise, $ZnEt_2$ consumes some surface $Cu^{(0)}$ during dissociative chemisorption in step 2b, but this is restored along with new $Cu^{(0)}$ in the subsequent step 1a of the Cu pulse. The transmetallation ALD cycle thus involves redox cycling of the entire Cu surface, with comproportionation to $Cu^{(I)}$ in steps 1b and 2b followed by reductive elimination of butane in steps 2a and 1a. Only the latter steps contribute to net growth of $Cu^{(0)}$ at the surface, which is likely to be a fraction of the overall Cu undergoing redox cycling. A similar picture has been described and quantified for redox ALD of noble metals[49].

The higher adsorption energies for the $Cu^{(I)}$ compounds of dmap ligands studied here suggest that a $Cu^{(I)}$ precursor should be preferred over a $Cu^{(II)}$ precursor. This holds true provided other requisite precursor properties are also fulfilled (e.g. volatility). There have been reports of $Cu^{(I)}$ compounds used as ALD precursors[15-16, 50] . In a recent study we have seen that $Cu^{(I)}$carbene compounds are promising precursors[38, 51]. However, $Cu^{(I)}$ compounds can disproportionate and deposit metal through a CVD pathway rather than through self-limiting ALD, so that stability may limit the use of $Cu^{(I)}$ compounds in ALD.

IV.(c). Interaction of co-reagent $ZnEt_2$ with the surface:

The advantages of $ZnEt_2$ as a reducing agent are that it is volatile and cheaply available. But the co-deposition of Zn with Cu makes it a poor choice. As seen from the

adsorption energy, $Zn^{(I)}$ has stronger adsorption than $Zn^{(II)}$. Thus, Zn may persist in (I) oxidation state instead of desorbing as ZnL_2, unless a ligand exchange reaction between the Cu and Zn takes place. The interaction of the $ZnEt_2$ fragments with a mixed surface of ligands from the precursor will be examined in another study later. The current study has clearly shown how CuEt fragments, formed either by ligand exchange or decomposition of $ZnEt_2$, are ultimately unstable against butane and $Cu^{(0)}$ formation.

IV. Conclusion:

We have computationally explored a part of the surface reactions during the transmetallation process for Cu ALD using DFT. Interactions of Cu(II) precursor molecules and the $ZnEt_2$ molecule with a bare copper surface have been studied (parts 1b and 2b, Figure 1). In this paper, we did not consider the interaction of the compounds in a mixed surface during the early part of the ALD pulse (as depicted in parts 1a and 2a). This is the subject of a forthcoming paper.

The general tendency of gas-phase $Cu^{(II)}$ complexes is to be planar. However, distortions occur due to bulky ligand groups interacting with each other. We see that precursors with less steric hindrance and planar geometry have strong adsorption to the surface, which is a positive indication for ALD. This is because the precursor can access the surface atoms relatively easily and form strong metallic bonds with the under coordinated surface Cu atoms. Ligands may also bond to surface Cu and/or dissociate from the adsorbate complex. At the end of the Cu precursor pulse, we predict that the surface will be covered in ligands attached to $Cu^{(I)}$ atoms. In all the cases studied here, we see that the adsorption does not depend so much on the electronegativity of the ligands as on the flexibility of the precursor complex and the orientation of alkyl substituents. Examining five precursors, we see that the $Cu(dmap)_2$ precursor adsorbs more strongly onto the surface due to the flexibility present in the ligand. Hence, we conclude that dmap-type ligands are best for the ALD of Cu and other transition

metals. $Cu(dmap)_2$ has also been previously used in experiments due to its high decomposition temperatures, low non-volatile residue and high sublimation rate[52]

$ZnEt_2$ is found to dissociate into a ZnEt fragment and Et on a bare copper surface. The ZnEt adsorbs to the copper surface more strongly than $ZnEt_2$ and then many Cu precursors. Therefore, impurities from residual ZnEt are inevitable during the ALD reaction unless there is complete exchange of Et with the ligands from the copper precursor. Hence, there is a need to find other reducing co-reagents that have less probability of producing impurities.

Achieving a surface covered with Cu_{surf}-Et is the key step for the deposition and growth of Cu(0), since a pair of these surface intermediates self-decomposes forming butane and liberating two electrons in order to deposit an atom of Cu metal. Overall in this transmetallation reaction it is the Et ligand that donates the electron to copper for its reduction to copper metal.

Acknowledgement:

We are grateful to Science Foundation Ireland for funding under the ALDesign project, grant number 09.IN1.I2628, http://www.tyndall.ie/aldesign.We have benefitted from discussions with Roger Nagle, Scott Clendenning and Harsono Simka of Intel Corporation and with Dirk Hagen of Tyndall National Institute.

Supporting Information Available: This information is available free of charge via the Internet at http://pubs.acs.org

TOC

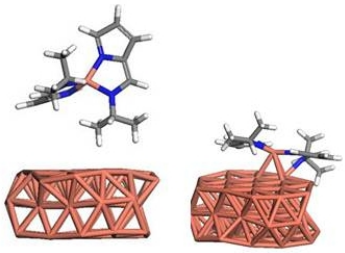

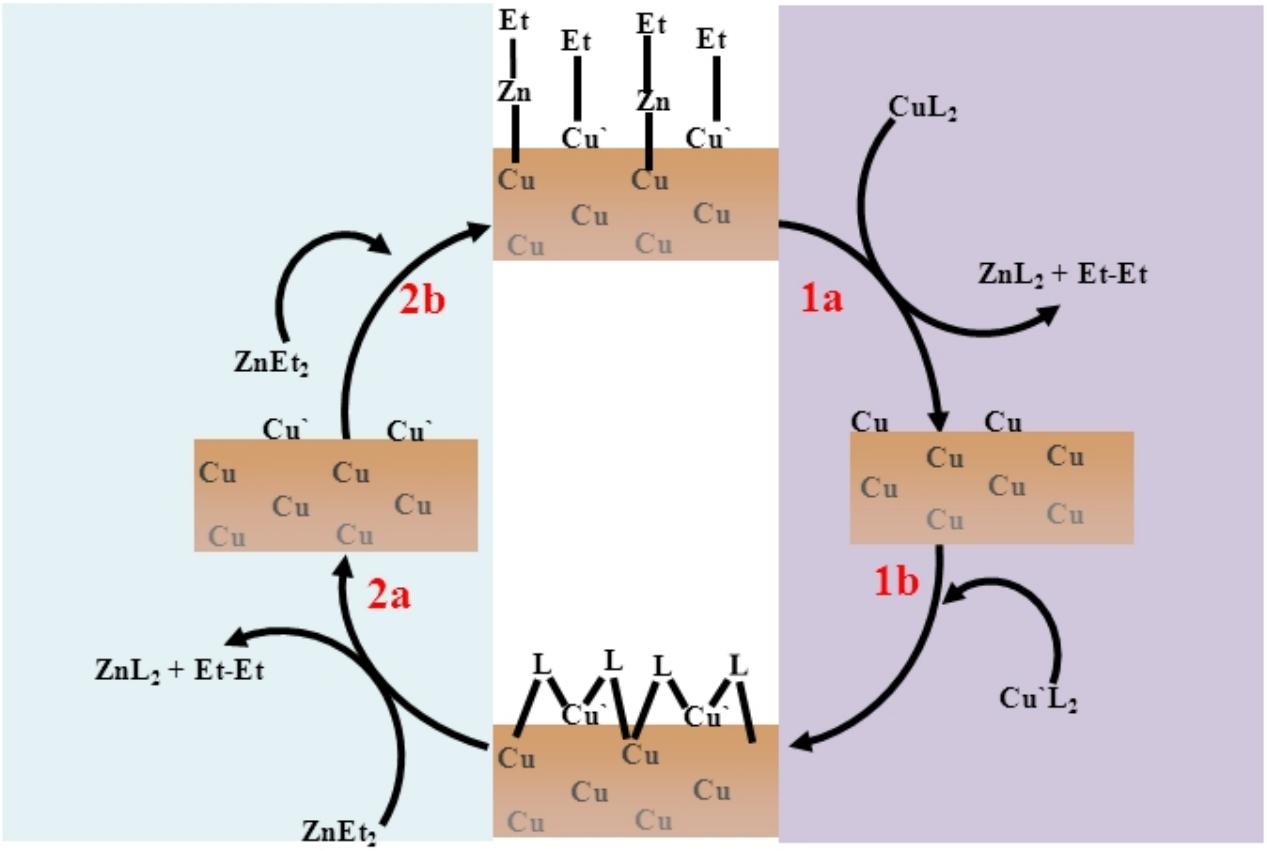

Figure 1: ALD cycle for proposed transmetallation reaction between copper precursor CuL_2 and reducing agent $ZnEt_2$. Each ALD pulse has been divided conceptually into two halves (a, b). The Cu precursor pulse on the right side with light pink shade is denoted as pulse 1 and the reducing agent pulse on the left side with light blue shade is denoted as pulse 2. Part 1a describes the reaction in a mixed surface between the incoming copper precursor and

previously adsorbed Et ligands. Part 1b describes the reaction when the Et ligand has been exhausted and fresh copper precursor adsorbs onto a bare copper surface. Part 2a involves the same reactions as 1a but during the reducing agent pulse when incoming $ZnEt_2$ interacts with previously adsorbed ligands from the Cu precursor. Part 2b shows the reaction when an excess of reducing agent adsorbs onto a bare copper surface.

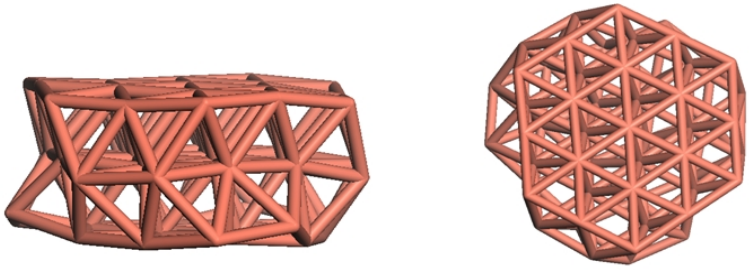

Figure 2: Side view and top view of the 3-layer deep Cu_{55} cluster, which is used as a model for the Cu(111) surface to investigate the adsorption of the copper precursors, intermediates and by-products.

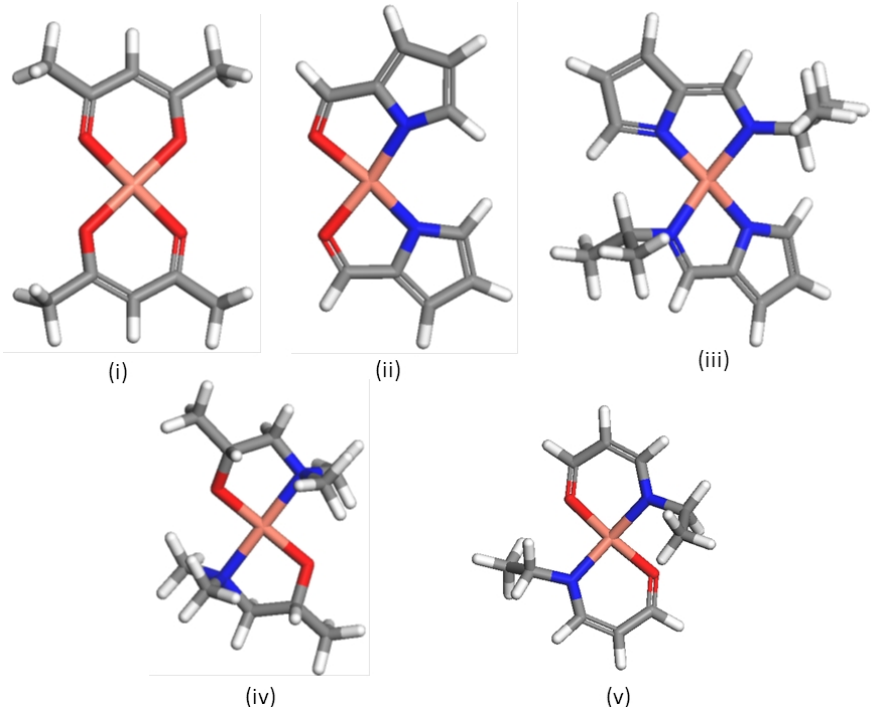

Figure 3: Lowest energy isomer computed in gas phase for potential ALD Cu precursors. (i) $Cu(acac)_2$ (ii) $Cu(PyrAld)_2$ (iii) $Cu(PyrIm^{iPr})_2$ (iv) $Cu(dmap)_2$ (v) $AbaCus^{(TM)}$. Structural

parameters are quoted in Table 1. Color code: Red = oxygen, Blue = nitrogen, Grey = carbon, White = hydrogen, Light brown = copper.

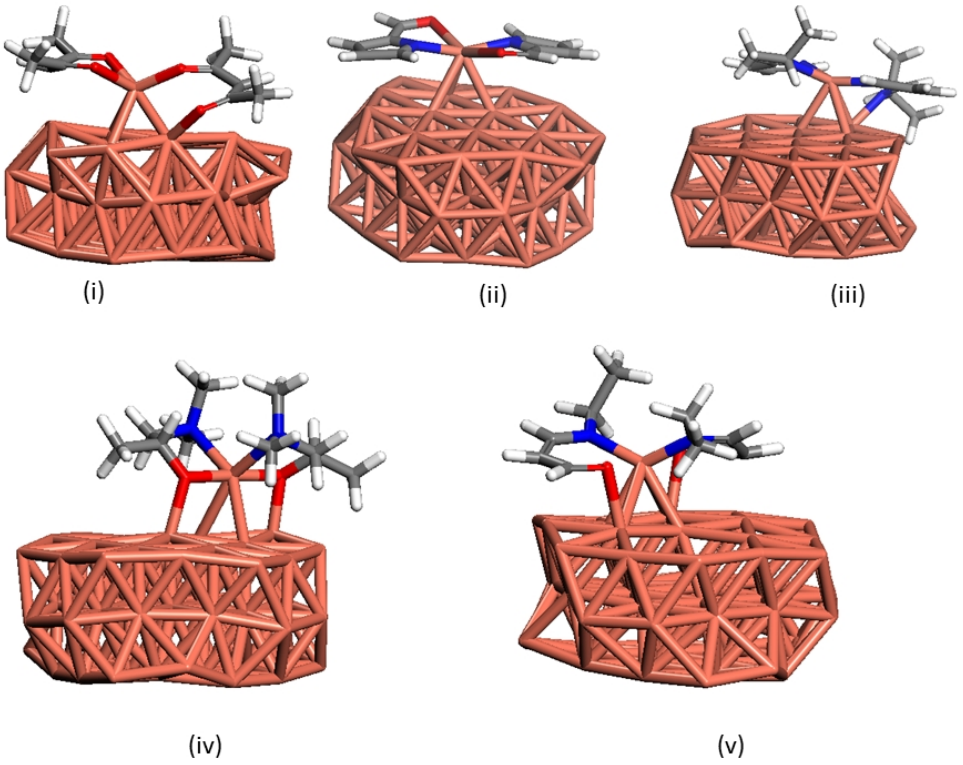

Figure 4: Optimized structures of precursors adsorbed onto the bare copper (111) surface. (i) $Cu(acac)_2$, (ii) $Cu(PyrAld)_2$, (iii) $Cu(PyrIm^{iPr})_2$, (iv) $Cu(dmap)_2$, (v) $AbaCus^{(TM)}$. The adsorption energy is in Table 2 and the structural changes in the precursor before and after adsorption in Table 1. Color code: Red = oxygen, Grey = carbon, White = hydrogen, Light brown = copper, Blue = nitrogen.

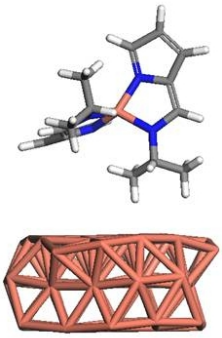

Figure 5: Lowest energy isomer of PyrIm^{iPr} precursor, which does not chemisorb in any orientation onto the copper surface due to steric hindrance (Figure 4 (iii)). Color code: Red = oxygen, Blue = nitrogen, Grey = carbon, White = hydrogen, Light brown = copper.

(i)

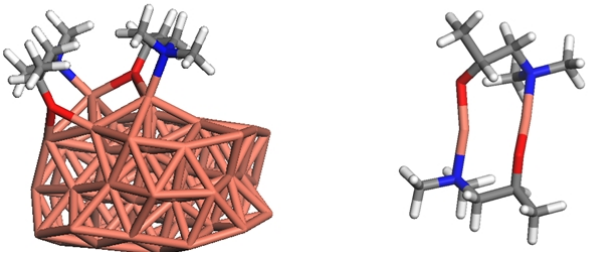

(ii)

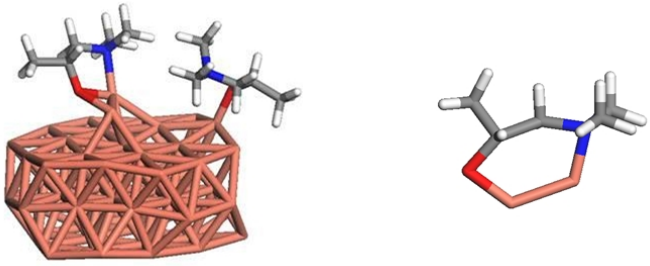

Figure 6: (i) The Cu_2L_2 (L=dmap) intermediate where there are two ligands, each attached to two adsorbed copper atoms. The corresponding gas phase structure is shown to the right. In the gas phase the distance between the two Cu atoms is $|Cu^{(I)}\text{-}Cu^{(I)}|_{(g)}$ = 2.48 Å and after adsorption onto the surface the distance is $|Cu\text{-}Cu|_{surf}$ = 3.55 Å. (ii) Cu_2L + L where the first

ligand is attached to two adsorbed copper atoms. The corresponding gas phase structure is also shown. In this case $|Cu\text{-}Cu|_{(g)}$ = 2.51 Å and $|Cu\text{-}Cu|_{surf}$ = 2.67 Å.

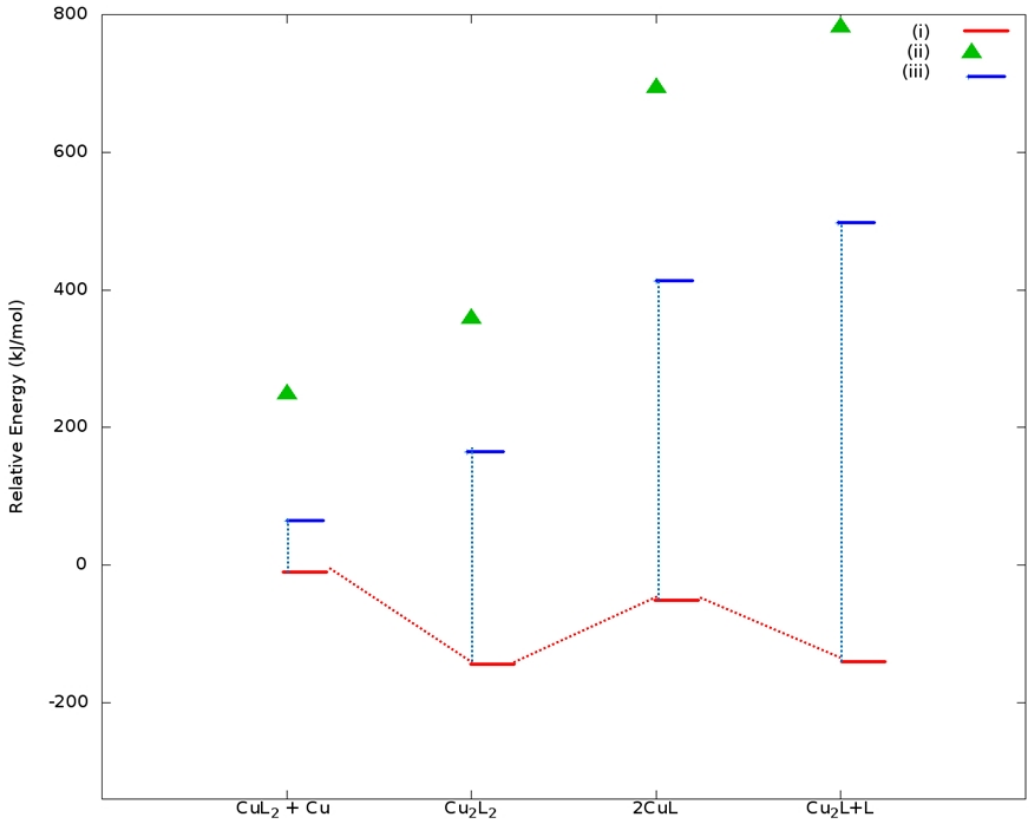

Figure 7: Energetics of surface intermediates during transmetallation when L = dmap is the ligand. The lower the energy in the graph, the more stable the system. (i) Red lines: The energy ΔE needed to transform the intermediate species into another on a bare copper surface. (ii) Green triangles: The desorption energy (ΔE_{des}) of the respective species into the gas phase relative to the red line. In the first structure the desorbed molecule is CuL_2, second Cu_2L_2, third CuL, and the last Cu_2L. (iii) Horizontal blue lines: The free energy (ΔG^{393}) including the entropy factor at 393 K needed for the species to desorb into the gas phase relative to the red line. Any particular intermediate has the probability of either desorption from the surface (red → blue) or else can form another surface intermediate (red → red). The data are presented in the supplementary information. No barriers have been computed.

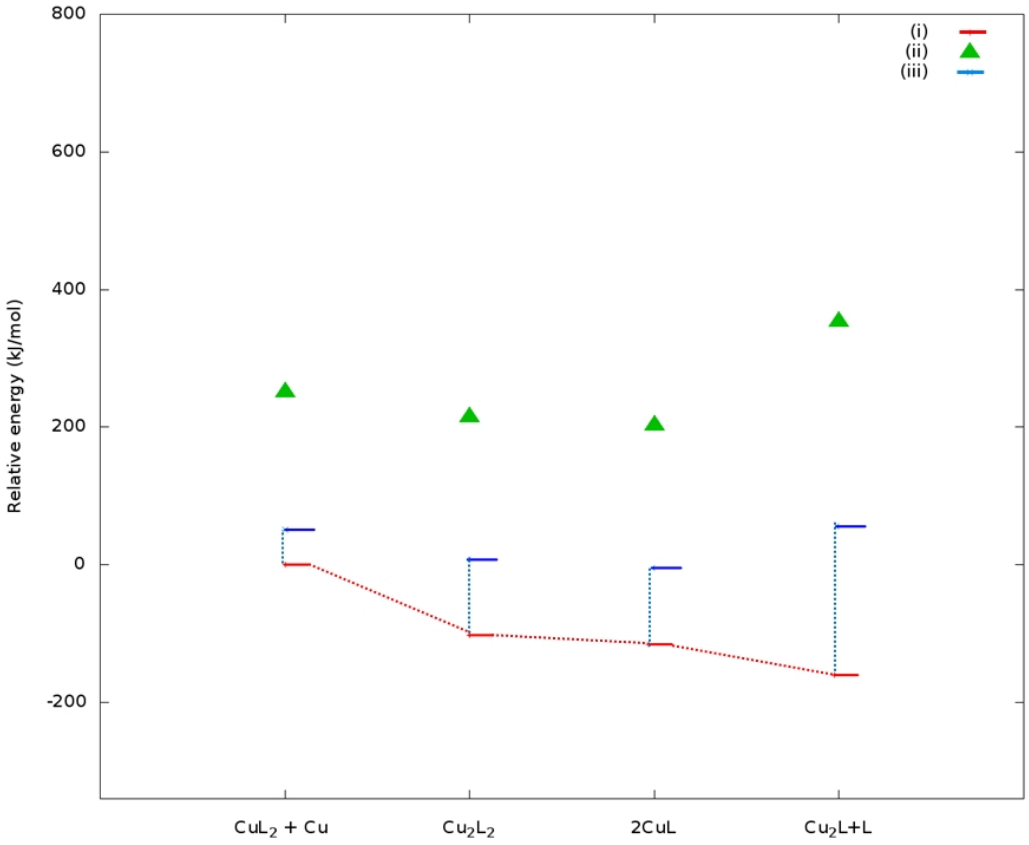

Figure 8: The graph shows similar results to that of Figure 7 but using L = PyrIm^{iPr} as the ligand.

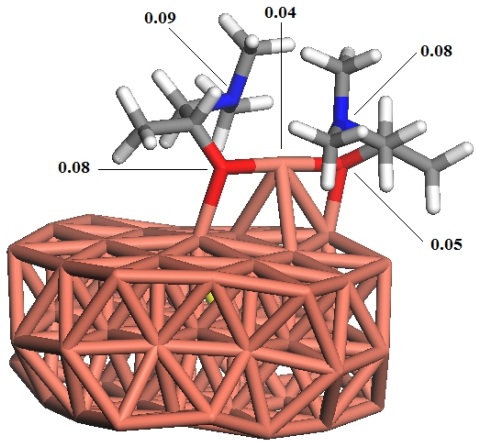

Figure 9: Optimized structure of Cu(dmap)$_2$ adsorbed on the (111) face of the copper coin. The differences in NPA charges on the Cu, O and N atoms between the gas phase precursor and the adsorbed precursor have been shown. The charges are more delocalized in the adsorbed structure compared to the gas phase. There are also changes in the surface with a

total change of charge ~0.40. Color code: Red = Oxygen, Blue = Nitrogen, Grey = Carbon, White = Hydrogen, Light brown = Copper.

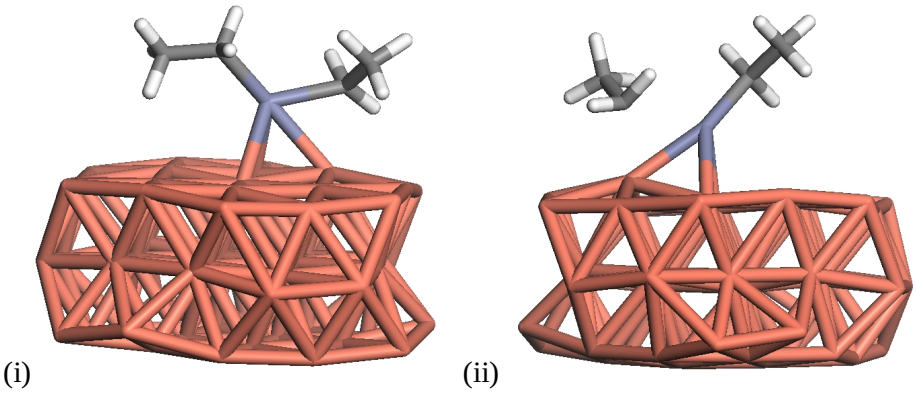

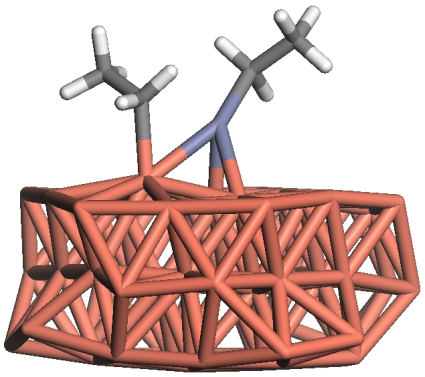

Figure 10: *Ab initio* Molecular Dynamics study for $ZnEt_2$ on Cu(111) surface. (i) Time t=0 shows $ZnEt_2$ attached to the surface. (ii) At time t=1.17 ps breaking of one C-Zn bond is apparent. Distance between C-Zn is 2.38 Å (C from the ethyl group). (iii) At time t=2.17ps, ZnEt and Et are separately attached to the copper surface. Structures (ii) and (iii) are not optimized geometries. Color code: brown=copper, blue-grey=zinc, grey=carbon and white=hydrogen.

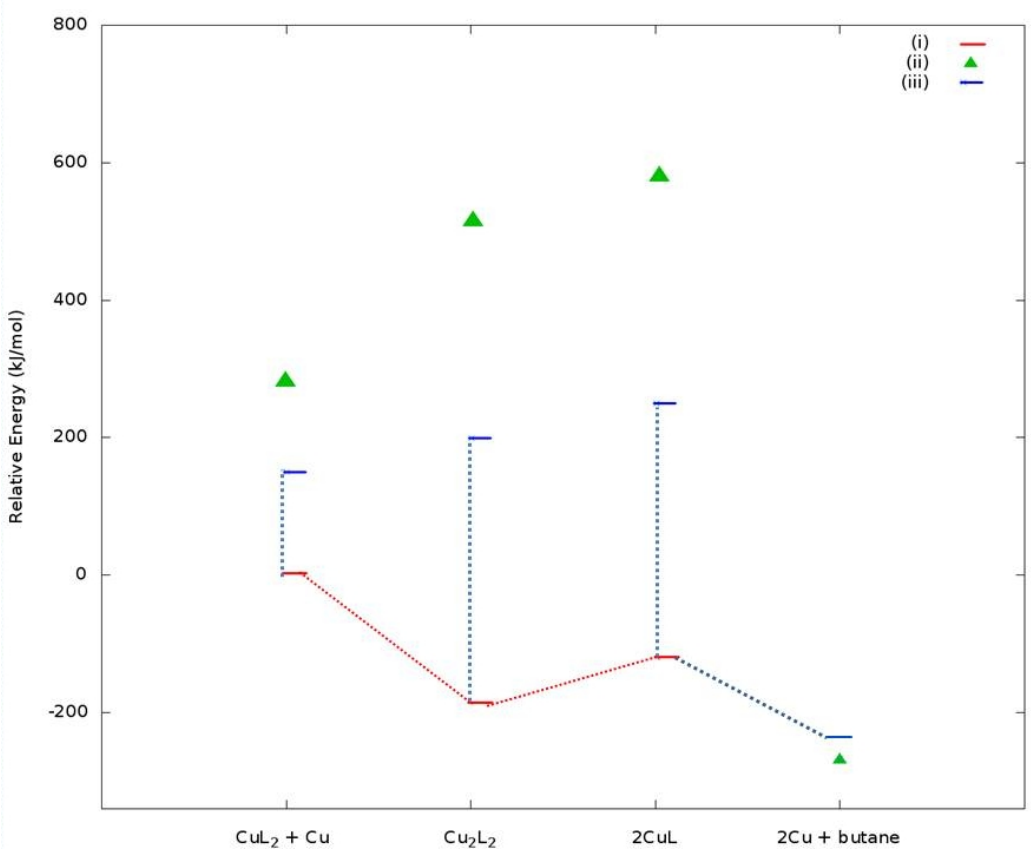

Figure 11: The graph shows similar results to that of Figure 7 but using L = Et as the ligand. The most important reaction shown in the graph is the interaction between two CuEt leading to the formation of butane with deposition of $Cu^{(0)}$. The same reaction can also take place when the Cu_2Et_2 dimer dissociates. The last intermediate has two new Cu atoms adsorbed to the surface and butane in gaseous form.

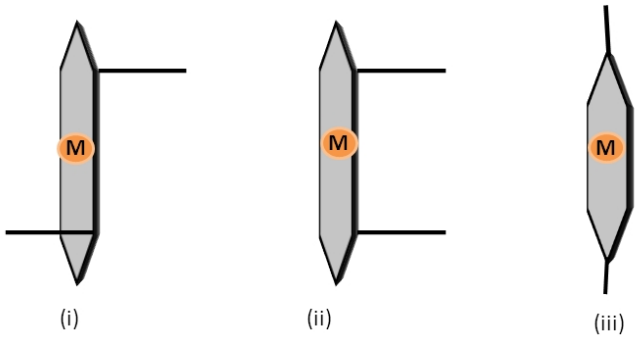

Figure 12: Schematic of substitution patterns on ligands affecting chemisorption of copper (II) precursors that are otherwise planar. In (i) the substitution is in opposite directions

perpendicular to the plane and there is no adsorption as the Cu_{pre} cannot access the surface. In (ii) the substitution is in one direction perpendicular to the plane, which makes the other plane available for adsorption. In (iii) the substitution is in the same plane as the copper complex, which does not hinder adsorption.

Table 1: Comparison of the structural properties of copper precursors when in the gas phase and after molecular adsorption onto the surface. Comparison has also been made with possible copper$^{(I)}$ intermediate. The dihedral angle is between the four coordinating atoms to the copper in the precursor, for example in $Cu(acac)_2$ the angle is between four oxygen atoms ∟O-O-O-O. The distance from the copper in the precursor to the nearest copper atom on the surface has also been noted and is represented as Cu-Cu. Here L = ligand in the precursor.

Precursors		CuL_2 in the gas phase	CuL_2 adsorbed onto the surface	$Cu^{(I)}L$ adsorbed onto the surface
$Cu(acac)_2$	Cu-O (Å)	1.95	2.10/2.13/4.08	2.05
	∟O-O-O-O (°)	0.1	9.73	6.57
	Cu-Cu (Å)	-	2.49	2.50
$Cu(PyrAld)_2$	Cu-N (Å)	1.97	1.95/1.96	2.03
	Cu-O (Å)	2.03	2.72/2.61	2.05
	∟O-N-O-N (°)	158.81	167.98	15.09
	Cu-Cu (Å)	-		2.48
$Cu(PyrIm)_2^R$ R=^{i}Pr	Cu-N_{Ar}(Å)	1.98	1.94	2.06/2.00
	Cu-N_{Ali}(Å)	2.04	1.96	2.00
	∟N-N-N-N (°)	38.73	71.41	19.78
	Cu-Cu (Å)	-	2.72	2.44

$Cu(dmap)_2$	Cu-O (Å)	1.91	1.95	2.13
	Cu-N(Å)	2.09	2.09	2.16
	∟O-N-O-N (°)	0.6	104.25	114.54
	Cu-Cu (Å)	-	2.62	2.46
AbaCuS	Cu-O (Å)	1.99	2.55	2.04
	Cu-N(Å)	1.99	2.03	2.02
	∟O-N-O-N (°)	131.39	141.15	0.03
	Cu-Cu (Å)	-	2.53	2.44
$CuEt_2$	Cu-C(Å)	1.97/1.96	2.00/1.99	-
	∟C-Cu-C (°)	137.95	152.12	-
	Cu-Cu (Å)	-	2.37	-

Table 2: Computed molecular adsorption energy (ΔE_{ad}) of copper precursors onto the copper surface along with the computed entropy contribution ($T\Delta S_{ad}$) of the molecules at T = 393 K. ΔG_{ad}^{393} denotes the free energy. All the values are in kJ/mol. Figure 3 shows the gas phase structure of precursor compounds and Figure 4 the adsorbed counterparts.

Ligand	ΔE_{ad}	$T\Delta S_{ad}$	ΔG_{ad}^{393}
acac	-258	-179	-79
PyrAld	-127	-171	44
$PyrIm^{iPr}$	-251	-200	-51
dmap	-249	-184	-64
AbaCus	-207	-175	-32
Et	-279	129	-150

Table 3: Computed adsorption energy (ΔE_{ad}), entropy contribution at 393 K ($T\Delta S_{ad}$) and free energy (ΔG^{393}_{ad}) of possible intermediates $Cu_2^{(I)}L_2$ on the Cu surface during transmetallation reaction. All the values are in kJ/mol.

Ligand	Molecule	ΔE_{ad}	$T\Delta S_{ad}$	ΔG^{393}_{ad}
dmap	$Cu^{(I)}_2(dmap)_2$	-504	-193	-311
$PyrIm^{iPr}$	$Cu^{(I)}_2(PyrIm^{iPr})_2$	-316	-207	-109
acac	$Cu^{(I)}_2(acac)_2$	-309	-186	-123
AbaCus	$Cu^{(I)}_2(Aba)_2$	-307	-186	-121

Table 4: Population analysis with NPA of the net charge in units of electronic charge on groups of atoms in the CuL_2 precursor, both in the gas phases (Figure 3) and then adsorbed onto the surface (Figure 4). Negative sign indicates negative charge. The same study has been done for the corresponding $Cu^{(I)}{}_2L_2$ surface intermediate. Cluster surface refers to the copper atoms of the whole coin.

Ligand	Gas Phase CuL_2			CuL_2 on the surface				Gas Phase Cu_2L_2				Cu_2L_2 intermediate on surface				
	Ligand 1	Ligand 2	Cu	Ligand 1	Ligand 2	Cu	Cluster surface	Ligand 1	Ligand 2	Cu^1	Cu^2	Ligand 1	Ligand 2	Cu^1	Cu^2	Cluster surface
$PyrIm^{iPr}$	-0.82	-0.82	1.64	-1.14	-0.75*	0.98	0.96	-0.66	-0.66	0.66	0.66	-0.92	-0.96	0.69	0.69	0.44
dmap	-0.56	-0.56	1.13	-0.88	-0.87	1.09	0.62	-0.64	-0.63	0.64	0.63	-0.69	-0.70	0.62	0.52	0.25
AbaCus	-0.59	-0.59	1.18	-0.94	-0.90	0.91	0.93	-0.68	-0.67	0.68	0.68	-0.86	-0.76	0.69	0.71	0.22

Reference:

1. (a) Kim, H., The application of atomic layer deposition for metallization of 65 nm and beyond. *Surface and Coatings Technology* **2006**, *200*, 3104-3111; (b) Merchant, S.; Kang, S.; Sanganeria, M.; van Schravendijk, B.; Mountsier, T., Copper interconnects for semiconductor devices. *JOM* **2001**, *53*, 43-48.
2. Yoo, H.-Y.; Chang, E.-G.; Kim, N.-H., Dual Damascene Process. *Transactions on Electrical and Electronic Materials* **2005**, *6*.
3. (a) Knisley, T. J.; Kalutarage, L. C.; Winter, C. H., Precursors and chemistry for the atomic layer deposition of metallic first row transition metal films. *Coordination Chemistry Reviews* **2013**, *257*, 3222-3231; (b) Leskelä, M.; Ritala, M., Atomic layer deposition chemistry: recent developments and future challenges. *Angewandte Chemie International Edition* **2003**, *42*, 5548-5554.
4. *International Technology Roadmap for Semiconductors* http://www.itrs.net/, 2011
5. George, S. M.; Ott, A. W.; Klaus, J. W., Surface Chemistry for Atomic Layer Growth. *The Journal of Physical Chemistry* **1996**, *100*, 13121-13131.
6. Pathangey, R. S. a. B., Atomic Layer Deposition of Copper Seed Layers. *Electrochemical and solid state letters* **2000**, *3*, 479-480.
7. Mårtensson, P.; Larsson, K.; Carlsson, J.-O., Atomic layer epitaxy of copper: an ab initio investigation of the CuCl/H2 process: II. Reaction energies. *Applied Surface Science* **1999**, *148*, 9-16.
8. Hsu, I. J.; McCandless, B. E.; Weiland, C.; Willis, B. G., Characterization of ALD copper thin films on palladium seed layers. *Journal of Vacuum Science & Technology A: Vacuum, Surfaces, and Films* **2009**, *27*, 660-667.
9. Knisley, T. J.; Ariyasena, T. C.; Sajavaara, T.; Saly, M. J.; Winter, C. H., Low Temperature Growth of High Purity, Low Resistivity Copper Films by Atomic Layer Deposition. *Chemistry of Materials* **2011**, *23*, 4417-4419.
10. Huo, J.; Solanki, R.; McAndrew, J., Characteristics of copper films produced via atomic layer deposition. *Journal of Materials Research* **2002**, *17*, 2394-2398.
11. Waechtler, T.; Ding, S.-F.; Hofmann, L.; Mothes, R.; Xie, Q.; Oswald, S.; Detavernier, C.; Schulz, S. E.; Qu, X.-P.; Lang, H.; Gessner, T., ALD-grown seed layers for electrochemical copper deposition integrated with different diffusion barrier systems. *Microelectronic Engineering* **2011**, *88*, 684-689.
12. Li, Z.; Gordon, R. G., Thin, Continuous, and Conformal Copper Films by Reduction of Atomic Layer Deposited Copper Nitride. *Chemical Vapor Deposition* **2006**, *12*, 435-441.
13. Kalutarage, L. C.; Martin, P. D.; Heeg, M. J.; Winter, C. H., Volatile and Thermally Stable Mid to Late Transition Metal Complexes Containing α-Imino Alkoxide Ligands, a New Strongly Reducing Coreagent, and Thermal Atomic Layer Deposition of Ni, Co, Fe, and Cr Metal Films. *Journal of the American Chemical Society* **2013**, *135*, 12588-12591.
14. Li, Z.; Barry, S. T.; Gordon, R. G., Synthesis and Characterization of Copper(I) Amidinates as Precursors for Atomic Layer Deposition (ALD) of Copper Metal. *Inorganic Chemistry* **2005**, *44*, 1728-1735.
15. Ma, Q.; Guo, H.; Gordon, R. G.; Zaera, F., Surface Chemistry of Copper(I) Acetamidinates in Connection with Atomic Layer Deposition (ALD) Processes. *Chemistry of Materials* **2011**, *23*, 3325-3334.
16. Lee, B. H.; Hwang, J. K.; Nam, J. W.; Lee, S. U.; Kim, J. T.; Koo, S.-M.; Baunemann, A.; Fischer, R. A.; Sung, M. M., Low-Temperature Atomic Layer Deposition of Copper Metal Thin Films: Self-Limiting Surface Reaction of Copper Dimethylamino-2-propoxide with Diethylzinc. *Angewandte Chemie International Edition* **2009**, *48*, 4536-4539.
17. (a) Bönnemann, H.; Richards, Ryan M., Nanoscopic Metal Particles – Synthetic Methods and Potential Applications. *European Journal of Inorganic Chemistry* **2001**, *2001*, 2455-2480; (b) Hambrock, J.; Schröter, M. K.; Birkner, A.; Wöll, C.; Fischer, R. A., Nano-Brass: Bimetallic Copper/Zinc

Colloids by a Nonaqueous Organometallic Route Using [Cu(OCH(Me)CH2NMe2)2] and Et2Zn as Precursors. *Chemistry of Materials* **2003**, *15*, 4217-4222.
18. (a) Vidjayacoumar, B.; Emslie, D. J. H.; Blackwell, J. M.; Clendenning, S. B.; Britten, J. F., Solution Reactions of a Bis(pyrrolylaldiminate)copper(II) Complex with Peralkyl Zinc, Aluminum, and Boron Reagents: Investigation of the Pathways Responsible for Copper Metal Deposition. *Chemistry of Materials* **2010**, *22*, 4854-4866; (b) Vidjayacoumar, B.; Emslie, D. J. H.; Clendenning, S. B.; Blackwell, J. M.; Britten, J. F.; Rheingold, A., Investigation of AlMe3, BEt3, and ZnEt2 as Co-Reagents for Low-Temperature Copper Metal ALD/Pulsed-CVD. *Chemistry of Materials* **2010**, *22*, 4844-4853.
19. Dey, G.; Elliott, S. D., Mechanism for the Atomic Layer Deposition of Copper Using Diethylzinc as the Reducing Agent: A Density Functional Theory Study Using Gas-Phase Molecules as a Model. *The Journal of Physical Chemistry A* **2012**, *116*, 8893-8901.
20. Mui, C.; Widjaja, Y.; Kang, J. K.; Musgrave, C. B., Surface reaction mechanisms for atomic layer deposition of silicon nitride. *Surface Science* **2004**, *557*, 159-170.
21. Elam, J. W.; Pellin, M. J.; Elliott, S. D.; Zydor, A.; Faia, M. C.; Hupp, J. T., Mechanism for zirconium oxide atomic layer deposition using bis(methylcyclopentadienyl)methoxymethyl zirconium. *Applied Physics Letters* **2007**, *91*, 253123-3.
22. Heyman, A.; Musgrave, C. B., A Quantum Chemical Study of the Atomic Layer Deposition of Al2O3 Using AlCl3 and H2O as Precursors. *The Journal of Physical Chemistry B* **2004**, *108*, 5718-5725.
23. Aaltonen, T.; Rahtu, A.; Ritala, M.; Leskelä, M., Reaction mechanism studies on atomic layer deposition of ruthenium and platinum. *Electrochemical and solid-state letters* **2003**, *6*, C130-C133.
24. Widjaja, Y.; Musgrave, C. B., Atomic layer deposition of hafnium oxide: A detailed reaction mechanism from first principles. *The Journal of Chemical Physics* **2002**, *117*, 1931-1934.
25. Elliott, S. D., Atomic-scale simulation of ALD chemistry. *Semiconductor Science and Technology* **2012**, *27*, 074008.
26. Pedersen, H.; Elliott, S., Studying chemical vapor deposition processes with theoretical chemistry. *Theor Chem Acc* **2014**, *133*, 1-10.
27. (a) Capelle, K., A bird's-eye view of density-functional theory. *Brazilian Journal of Physics* **2006**, *36*, 1318-1343; (b) Szabo, A.; Ostlund, N. S., *Modern Quantum Chemistry- Introduction to advanced electronic structure theory*; Dover Publications, INC.: Mineola, New York, 1982.
28. Olivier, S.; Ducéré, J.-M.; Mastail, C.; Landa, G.; Estève, A.; Rouhani, M. D., Insights into Crystalline Preorganization of Gas-Phase Precursors: Densification Mechanisms. *Chemistry of Materials* **2008**, *20*, 1555-1560.
29. Shirazi, M.; Elliott, S. D., Multiple Proton Diffusion and Film Densification in Atomic Layer Deposition Modeled by Density Functional Theory. *Chemistry of Materials* **2013**, *25*, 878-889.
30. Mikko Ritala, M. L., Handbook of Thin Film Materials, Chapter 2. *Academic Press ISBN 0-12-512909-2*, *1*, 103-159.
31. (a) Ahlrichs, R.; Elliott, S. D.; Huniar, U., Quantum chemistry: Large molecules - Small computers. *Berichte Der Bunsen-Gesellschaft-Physical Chemistry Chemical Physics* **1998**, *102*, 795-804; (b) Schafer, A.; Huber, C.; Ahlrichs, R., Fully optimized contracted Gaussian basis sets of triple zeta valence quality for atoms Li to Kr. *The Journal of Chemical Physics* **1994**, *100*, 5829-5835.
32. Perdew, J. P.; Burke, K.; Ernzerhof, M., Generalized Gradient Approximation Made Simple. *Physical Review Letters* **1996**, *77*, 3865.
33. (a) Eichkorn, K.; Weigend, F.; Treutler, O.; Ahlrichs, R., Auxiliary basis sets for main row atoms and transition metals and their use to approximate Coulomb potentials. *Theoretical Chemistry Accounts: Theory, Computation, and Modeling (Theoretica Chimica Acta)* **1997**, *97*, 119-124; (b) Sierka, M.; Hogekamp, A.; Ahlrichs, R., Fast evaluation of the Coulomb potential for electron densities using multipole accelerated resolution of identity approximation. *The Journal of Chemical Physics* **2003**, *118*, 9136-9148.
34. (a) Weigend, F.; Häser, M.; Patzelt, H.; Ahlrichs, R., RI-MP2: optimized auxiliary basis sets and demonstration of efficiency. *Chemical Physics Letters* **1998**, *294*, 143-152; (b) Hattig, C., Optimization of auxiliary basis sets for RI-MP2 and RI-CC2 calculations: Core-valence and quintuple-[small zeta]

basis sets for H to Ar and QZVPP basis sets for Li to Kr. *Physical Chemistry Chemical Physics* **2005**, *7*, 59-66.
35. Grimme, S., Semiempirical GGA-type density functional constructed with a long-range dispersion correction. *Journal of computational chemistry* **2006**, *27*, 1787-1799.
36. Dey, G.; Elliott, S., Copper(I) carbene hydride complexes acting both as reducing agent and precursor for Cu ALD: a study through density functional theory. *Theor Chem Acc* **2013**, *133*, 1-7.
37. Larsson, J. A.; Elliott, S. D.; Greer, J. C.; Repp, J.; Meyer, G.; Allenspach, R., Orientation of individual C_{60} molecules adsorbed on Cu(111): Low-temperature scanning tunneling microscopy and density functional calculations. *Physical Review B* **2008**, *77*, 115434.
38. Coyle, J. P.; Dey, G.; Sirianni, E. R.; Kemell, M. L.; Yap, G. P. A.; Ritala, M.; Leskelä, M.; Elliott, S. D.; Barry, S. T., Deposition of Copper by Plasma-Enhanced Atomic Layer Deposition Using a Novel N-Heterocyclic Carbene Precursor. *Chemistry of Materials* **2013**, *25*, 1132-1138.
39. (a) Crispin, X.; Bureau, C.; Geskin, V. M.; Lazzaroni, R.; Salaneck, W. R.; Brédas, J. L., Chemisorption of acrylonitrile on the Cu(100) surface: A local density functional study. *The Journal of Chemical Physics* **1999**, *111*, 3237-3251; (b) Crispin, X.; Geskin, V.; Crispin, A.; Cornil, J.; Lazzaroni, R.; Salaneck, W. R.; Brédas, J.-L., Characterization of the Interface Dipole at Organic/ Metal Interfaces. *Journal of the American Chemical Society* **2002**, *124*, 8131-8141; (c) Crispin, X.; Bureau, C.; Geskin, V.; Lazzaroni, R.; Brédas, J.-L., Local Density Functional Study of Copper Clusters: A Comparison between Real Clusters, Model Surface Clusters, and the Actual Metal Surface. *European Journal of Inorganic Chemistry* **1999**, *1999*, 349-360.
40. Deglmann, P.; May, K.; Furche, F.; Ahlrichs, R., Nuclear second analytical derivative calculations using auxiliary basis set expansions. *Chemical Physics Letters* **2004**, *384*, 103-107.
41. Cioslowski, J., A new population analysis based on atomic polar tensors. *Journal of the American Chemical Society* **1989**, *111*, 8333-8336.
42. Reed, A. E.; Weinstock, R. B.; Weinhold, F., Natural population analysis. *The Journal of Chemical Physics* **1985**, *83*, 735-746.
43. Liu, Y.-F.; Xia, H.-T.; Yang, S.-P.; Wang, D.-Q., Bis{[mu]-6,6'-dimethoxy-2,2'-[propane-1,2-diylbis(iminomethylene)]diphenolato}bis[aquacopper(II)] dihydrate. *Acta Crystallographica Section C* **2008**, *64*, m91-m93.
44. Kanda, H.; Narumi, Y.; Hosokoshi, Y.; Suzuki, T.; Kawata, S.; Kindo, K.; Inoue, K.; Kaizaki, S., Synthesis, magnetic properties and MCD spectra of a four coordinate copper(II) complex with two chelated phenolate-substituted imino nitroxides. *Inorganica Chimica Acta* **2004**, *357*, 3125-3133.
45. Becker, R.; Devi, A.; Weiß, J.; Weckenmann, U.; Winter, M.; Kiener, C.; Becker, H. W.; Fischer, R. A., A Study on the Metal Organic CVD of Pure Copper Films from Low Cost Copper(II) Dialkylamino-2-propoxides: Tuning the Thermal Properties of the Precursor by Small Variations of the Ligand. *Chemical Vapor Deposition* **2003**, *9*, 149-156.
46. Puurunen, R. L., Surface chemistry of atomic layer deposition: A case study for the trimethylaluminum/water process. *Journal of Applied Physics* **2005**, *97*, 121301.
47. Zydor, A.; Elliott, S. D., TiCp (OMe) 3 versus Ti (OMe) 4 in Atomic Layer Deposition of TiO2 with WaterAb Initio Modelling of Atomic Layer Deposition Surface Reactions. *Journal of Nanoscience and Nanotechnology* **2011**, *11*, 8089-8093.
48. Zydor, A.; Kessler, V. G.; Elliott, S. D., First principles simulation of reaction steps in the atomic layer deposition of titania: dependence of growth on Lewis acidity of titanocene precursor. *Physical Chemistry Chemical Physics* **2012**, *14*, 7954-7964.
49. Elliott, S. D., Mechanism, Products, and Growth Rate of Atomic Layer Deposition of Noble Metals. *Langmuir* **2010**, *26*, 9179-9182.
50. Hagen, D. J.; Connolly, J.; Nagle, R.; Povey, I. M.; Rushworth, S.; Carolan, P.; Ma, P.; Pemble, M. E., Plasma enhanced atomic layer deposition of copper: A comparison of precursors. *Surface and Coatings Technology* **2013**, *230*, 3-12.

51. Coyle, J. P.; Kurek, A.; Pallister, P. J.; Sirianni, E. R.; Yap, G. P. A.; Barry, S. T., Preventing thermolysis: precursor design for volatile copper compounds. *Chemical Communications* **2012**, *48*, 10440-10442.
52. Kalutarage, L. C.; Clendenning, S. B.; Winter, C. H., Low-Temperature Atomic Layer Deposition of Copper Films Using Borane Dimethylamine as the Reducing Co-reagent. *Chemistry of Materials* **2014**, *26*, 3731-3738.